3rd International Conference on Materials Processing and Characterisation (ICMPC 2014)

Microstructural and mechanical properties of walking friction stir spot welded AA 6061-T6 sheets

S.Venukumar[a], Bibin Baby[a], S.Muthukumaran*[a] and Satish V. Kailas[b]

[a]Department of Metallurgical and Materials Engineering, National Institute of Technology,
Tiruchirappalli-620015, Tamil Nadu, India
[b]Department of Mechanical Engineering, Indian Institute of Science, Bangalore 560012, India

Abstract

In order to increase the strength of the joint, a novel spot welding process named walking friction stir spot welding(WFSSW) has been applied for AA 6061-T6 joints using a tool movement over a distance of 15 mm. This process was carried out for four different tool rotational speeds and a better static shear strength was achieved at a tool rotational speed of 900 rpm. Macro and microstructural analysis were made in order to analyze the local material microstruture evolution. The variation of microhardness in different regions of the weld was analyzed. Fatigue tests were conducted on lap-shear specimens at a stress ratio of R=0.1. Two different fracture modes were observed under both quasi-static and cyclic loading conditions. The fracture surfaces were analyzed by using optical and scanning electron micrographs.

1. Introduction

In recent years, lightening in the transportation vehicles, such as automobile, train, airplane, is strongly desired from the viewpoint both of energy saving and avoidance against environmental pollution.

* Corresponding author.. Tel.: +91-9442069381; fax: 91-431-2500133.
  E-mail address: smuthu@nitt.edu

While the AA 6061 is widely utilized for the structural components in these vehicles extensively because of their properties such as medium strength, formability, corrosion resistance and low cost (Agarwal et al., 2003; Venukumar et al., 2013). Recently, a variant of the "linear" Friction stir welding called Friction stir spot welding (FSSW) has been developed and implemented in automotive industry as a replacement of resistance spot welding for aluminum. Mazda corporation of Japan proposed the friction stir spot welding, which has been successfully applied to the production of hood and rear door of the sport vehicle Mazada RX-8 (William, 2007; Mazda, 2003). The FSSW process consists of three stages; plunging and stirring and retraction. The process starts with spinning the tool with high rotational speed and plunging it into the weld spot until shoulder contacts the top surface of the work piece. Then, the stirring phase enables the materials of the two workpieces mix together with a strong compressive forging pressure. Lastly, once a predetermined penetration is reached, the process stops and the tool retracts from the workpiece. In this work an attempt has been made to weld AA 6061-T6 sheets by moving the tool before drawing it out. As the tool moves, it has been named as walking friction stir spot welding(WFSSW). The difference between conventional FSSW and walking FSSW process is that in walking FSSW(Fig. 1) the tool moves a distance along the longitudinal direction after completely plunging. This distance is called walking length. The steps involved in the WFSSW are (1) plunging, in which the tool is plunged into the work pieces. (2) Stirring, in this the tool rotation stir the metal producing a weld. (2) Tool movement in longitudinal direction, which produces more bond area. (4) Drawing out, in this, tool is drawn out leaving a hole in the weld.

While a paper on the joining of 5052 aluminum alloys using walking friction stir spot welding have been recently reported (Zhang et al., 2011), only limited studies have been done on lap shear strength and particularly fatigue resistance of these joints, a topic of vital importance for ensuring safe and reliable applications (Chowdhury et al., 2012). Fatigue behaviour of a spot friction welds is extremely dependent on process parameters. This dependence may be from variation in speed, depth of plunge, dwell time, and tool configuration employed to create the weld (Jordon et al., 2010; Lin et al., 2008). Tozaki et al.(Tozaki et al., 2007) stated that the shear strength decreased with increasing tool rotational speed. But Lathabai et al. (Lathabai et al., 2006) reported that with increasing tool rotational speed the static shear strength increased and then decreased in the AA6061-T5 friction stir spot weld joints (Arul et al., 2008). Tran et al. (Tran et al., 2008) indicated that the failure modes of the 5754 and 6111 spot friction welds under quasi-static and cyclic loading conditions are quite different.

Due to advantage of this technique, such as the resulting better static shear strength and fatigue properties, WFSSW has been successfully used for joining AA 6061-T6 sheets. This paper contains microstructures, mechanical properties, fracture and fatigue behaviours of the walking friction stir spot welds. The fracture surface of the failed quasi-static and fatigue specimens were analysed by using the optical and scanning electron microscope.

2. Experimental Procedure

In the present study, aluminum 6061-T6 rolled sheets of 2 mm thickness were chosen, and their chemical composition is listed in Table 1. The work piece length, width and overlapping length are 100 mm, 30 mm and 30 mm respectively. The welds were made by using a modified milling machine and the tool geometry consists of a shoulder of 18 mm diameter and a pin of 5 mm diameter. Four different values of the tool rotational speeds, namely, 900, 1120, 1400 and 1800 rpm, were chosen, and the test was repeated three times at each speed. All welds are made under the following process parameters: plunge speed of 30 mm/min, walking length of 15 mm, dwell time of 2 s and shoulder plunge depth of 0.3 mm.

Macrostructural study was carried out by using optical microscope for getting different regions of friction stir spot welded specimen. For observation of weld macrostructures, specimens were etched with the Tucker's reagent (3 ml HNO_3, 9 ml HCL, 3 ml HF and 5 ml water). The etchant time used was 15-20 seconds. Microstructural studies were carried out by using optical microscope and specimens were Poulton reagent (30ml HCl, 40ml HNO_3, 2.5ml HF, 12 gm CrO_3, 42.5ml H_2O) and the etching time used was 15-20 seconds. The Vickers microhardness test was performed on the cross-section of the FSSW samples using a 500 g load for 20 s to obtain the hardness profiles. The lap shear samples were prepared according to the dimensions shown in Fig. 2. They were tested, by using a tensile testing machine at a monotonic displacement rate of 0.01 mm/s. The load and displacement were simultaneously recorded during the test. The lap shear strength was obtained by averaging the strengths of three individual specimens, which were welded with identical welding parameters.

A BiSS nano universal testing machine was used to conduct the fatigue tests. The specimens were subjected to constant amplitude sinusoidal loading, with a loading ratio $R=P_{min}/P_{max}$ of 0.1, and a frequency of 4 Hz. The maximum allowable load for the fatigue test is 4.5 KN, and this value corresponds to two-thirds of the peak load (Malafaia et al., 2010). The fracture surfaces of the WFSSW joints after the fatigue tests were analyzed in detail, using the scanning electron microscope. A graph was plotted to show the experimental results for the walking spot friction welds under cyclic loading conditions.

Table 1 Chemical composition (weight in %) of Al6061-T6 alloy sheets used in this work

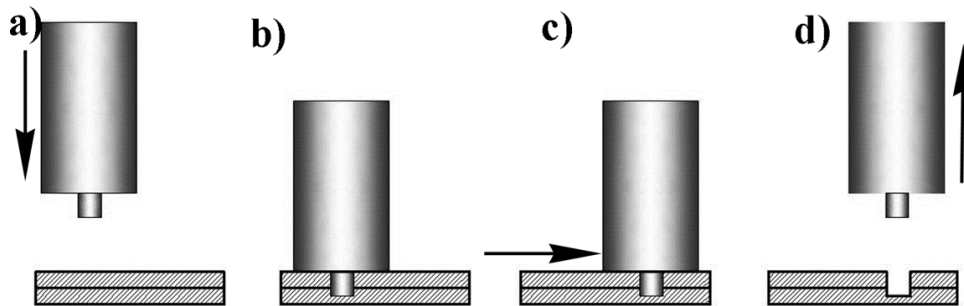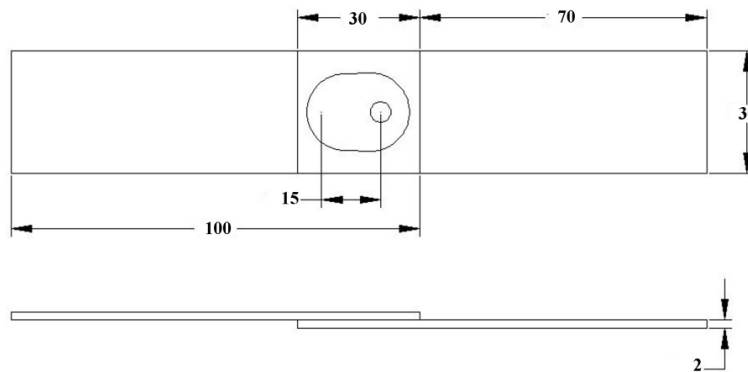|	
Mg	0.708
Si	0.434
Fe	0.497
Cu	0.164
Cr	0.148
Mn	0.0971
Ti	0.0495
Zn	0.0042
Al	Remaining

Fig. 1. Schematic representation of WFSSW.

Fig. 2. Schematic representation of lap shear specimen.

3. Results and Discussion

The static shear strengths of the welds made by the WFSSW at different tool rotational speeds, are shown in Fig. 3. As tool rotational speed increases, the static shear strength is lowered, so that heat input is also decreased. Then, the material plasticity does not reach the required extent. Fig. 3 clearly shows the variation of static shear strength by increasing the speed. The maximum static shear strength 8416 N occurs at a tool rotational speed of 900 rpm.
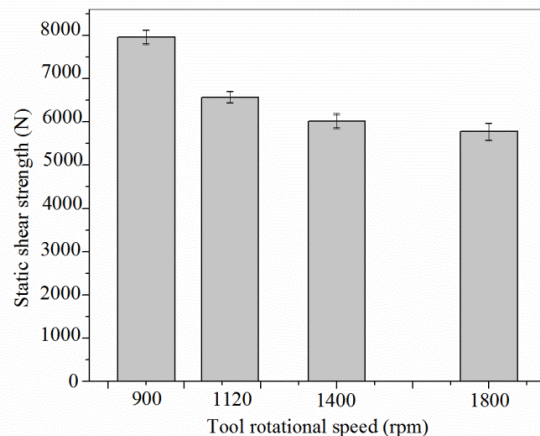

Fig. 3. Static shear strength of WFSSW joints made by WFSSW.

Fig. 4a shows a typical macrostructures of the cross-section at different regions of WFSSW joint made at a tool rotational speed of 900 rpm. In the cross-section, the left and right sides of the weld centre are related to the retreating and advancing sides of the rotating tool, respectively. The macrostructure of joint can be classified into three distinct regions including the stir zone (HAZ) was not clearly observed.

Fig. 4 shows the microstructure at different regions. More grain refinement can be observed in stir zone (SZ). Since SZ is adjacent to the keyhole, most of the stirring action takes place in this region. The grains in this region are subjected to high plunging action and undergo dynamic recrystallization due to high temperature produced by frictional heat and hence very fine equiaxed grains with the average size of 15 μm is obtained. The TMAZ (Fig. 4c) consists of elongated grains oriented to certain direction caused by deformation by the tool. This region was also exhibited to high temperatures, however no or only limited recrytallization took place.

3.1 Microhardness

Fig. 5 shows the hardness distribution of WFSSW joint made at a tool rotational speed of 900 rpm. The hardness of aluminum alloy showed W-shape distribution. Reduction of hardness was observed outside of stir zone and minimum hardness was approximately 47 HV. The hardness increase in SZ is due to fine grains and precipitates.
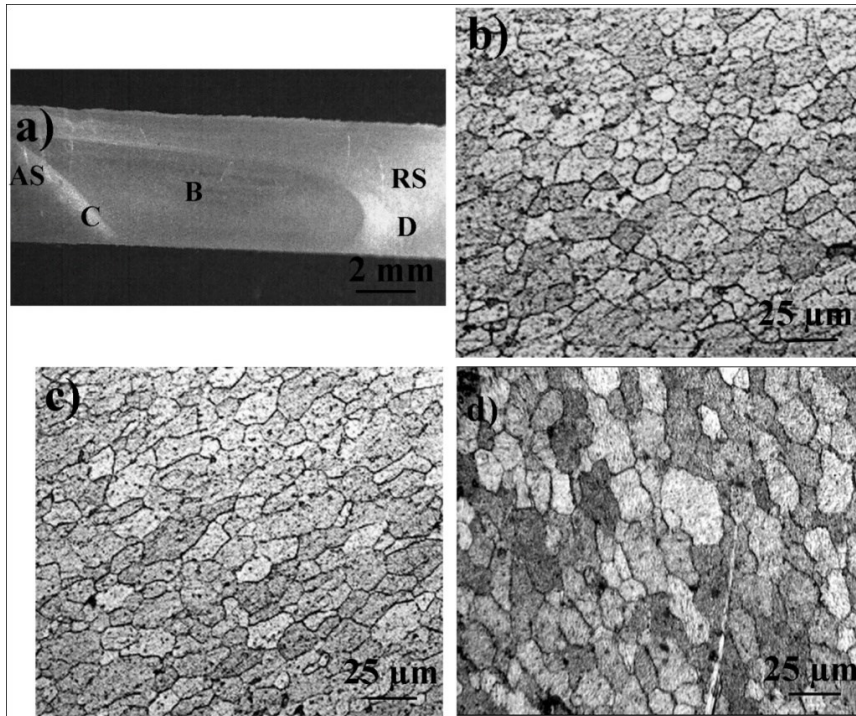
Fig. 4. (a) Macroscopic appearance of the WFSSW joint; Microstructures in WFSSW (b) SZ (c) TMAZ (d) BM.
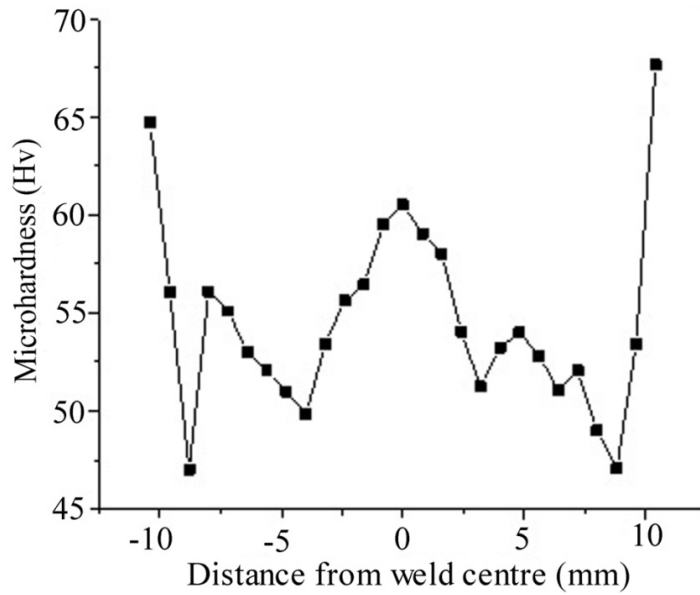

Fig. 5. Hardness profile of WFSSW joint across the weld interface.

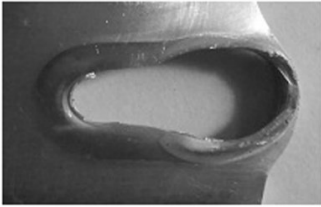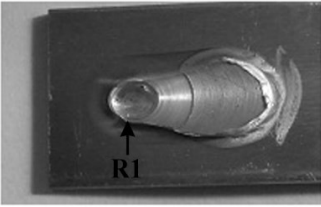**3.2 Failure modes under quasi-static and cyclic loading conditions**

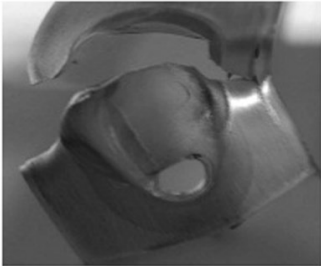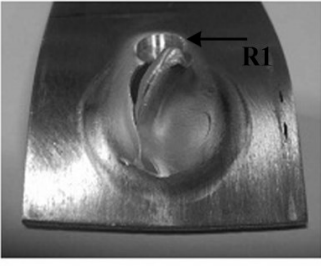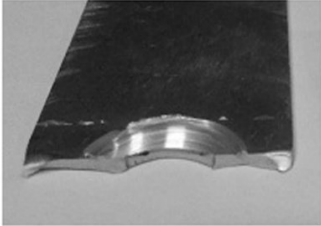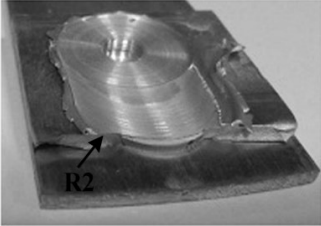| Failure modes under	Upper sheet	Lower sheet
Quasi-static conditions		
Cyclic loading conditions Load range (N)		
4150 N		
1800 N		

Fig. 6. Modes of fracture under quasi-static and cyclic loading conditions.

The experiments were performed under quasi-static and cyclic loading conditions. Based on the experimental results, the failed walking friction stir spot welds under quasi-static loading conditions show one failure mode. The failed walking friction stir spot welds under cyclic loading conditions with the fatigue lives from 10^3 to 10^4 show similar failure mode. The failed walking friction stir spot welds under cyclic loading conditions with the fatigue lives from 10^4 to 10^5 show another failure mode. Subsequently, a macroscopic appearance of the failure modes under loading conditions of quasi-static, low-cycle fatigue (lives of 10^3 to 10^4), and high-cycle fatigue (lives of 10^4 to 10^5) is presented in Fig. 6. The fracture surface of the lower sheet under low cyclic loading conditions (Fig. 6), a crack (marked as R1) seems to emanate from the outside of stir zone and propagate little bit upwards. Then a shear failure passes at the end of R1. The failure then propagates along the nugget circumference and, eventually, the lower sheet is ruptured with some part of the nugget. A similar failure mode is observed under quasi-static loading conditions. Fig. 6 shows the upper sheet of a failed lap shear specimen at the fatigue life of nearly 10^5 (1800 N). It is noted that fatigue crack is initiated by R2 and propagated through the transverse direction in the upper sheet at the higher loads. This indicates that the transition of fatigue fracture mechanism depending on load level.

Fig. 7 shows a scanning electron micrograph of the fatigue fracture surfaces at P_{max}=4500 N and N_f=4.9×10^4 observed on lower aluminum sheet. Figs. 7 (a1) and (b1) are the magnified views at the locations "A1" and "B1" in Figs 7 (a) and (b), respectively. As mentioned earlier, fatigue fracture occurred through the interface. It can be clearly identified that shear fracture has taken place along the boundary between the upper and lower sheets along the periphery of the nugget and the two sheets has been completely sheared off.
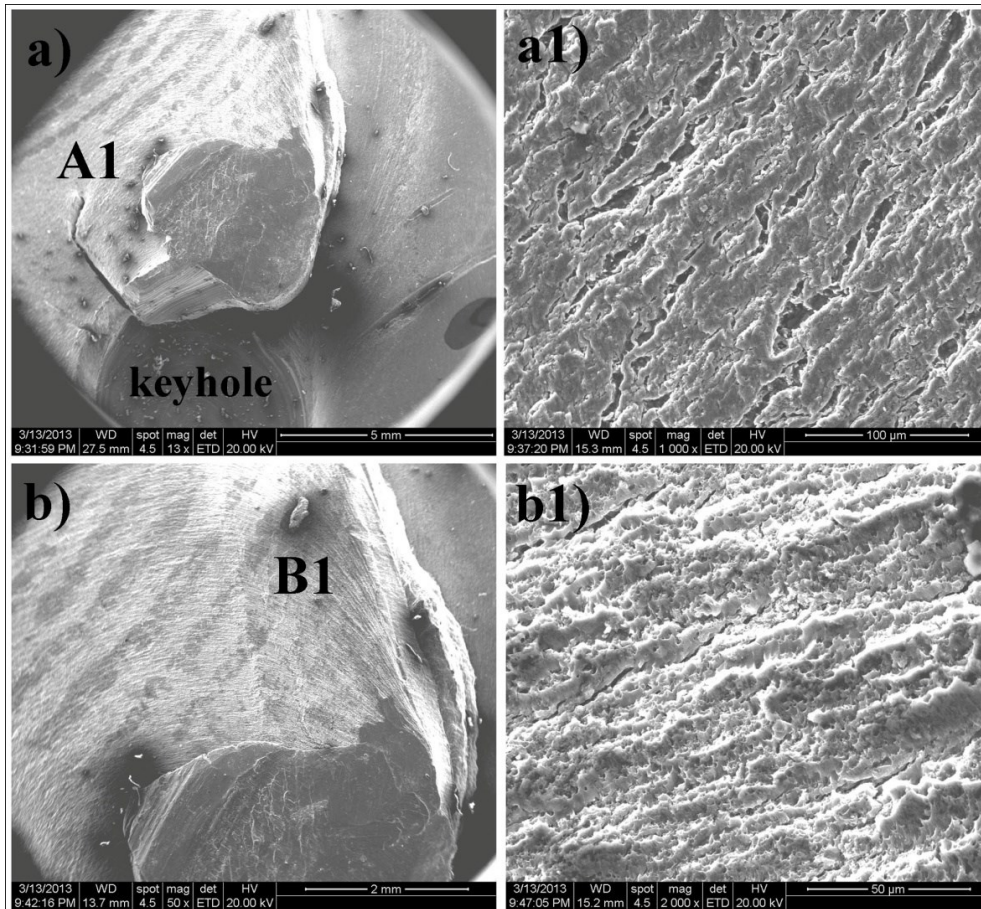

Fig. 7. Typical SEM micrographs of fracture surfaces in WFSSW joint (a), (b) shear fracture surface of lower sheet, (a1) and (b1) magnified views at points at A, B in (a) and (b) respectively.

Fig. 8 shows a scanning electron micrograph of the fatigue fracture surfaces at P_{max}= 2000 N and N_f=1.9×10^5 observed on cross sectional area of upper sheet. Figs. 8(a1), (b1) and (c1) are the magnified views at the locations "A1", "B1" and "C1" in figures (a), (b) and (c) respectively. The fatigue striations can be clearly observed in "A1" and "B1" regions. Figs. 8(a) and 8(b), revealed that the fatigue crack propagated in a semicircular path, starting from the top center of the nugget weld. In the end, the dimple surface was observed in "C1" region and hence, the static fracture observed at this region.
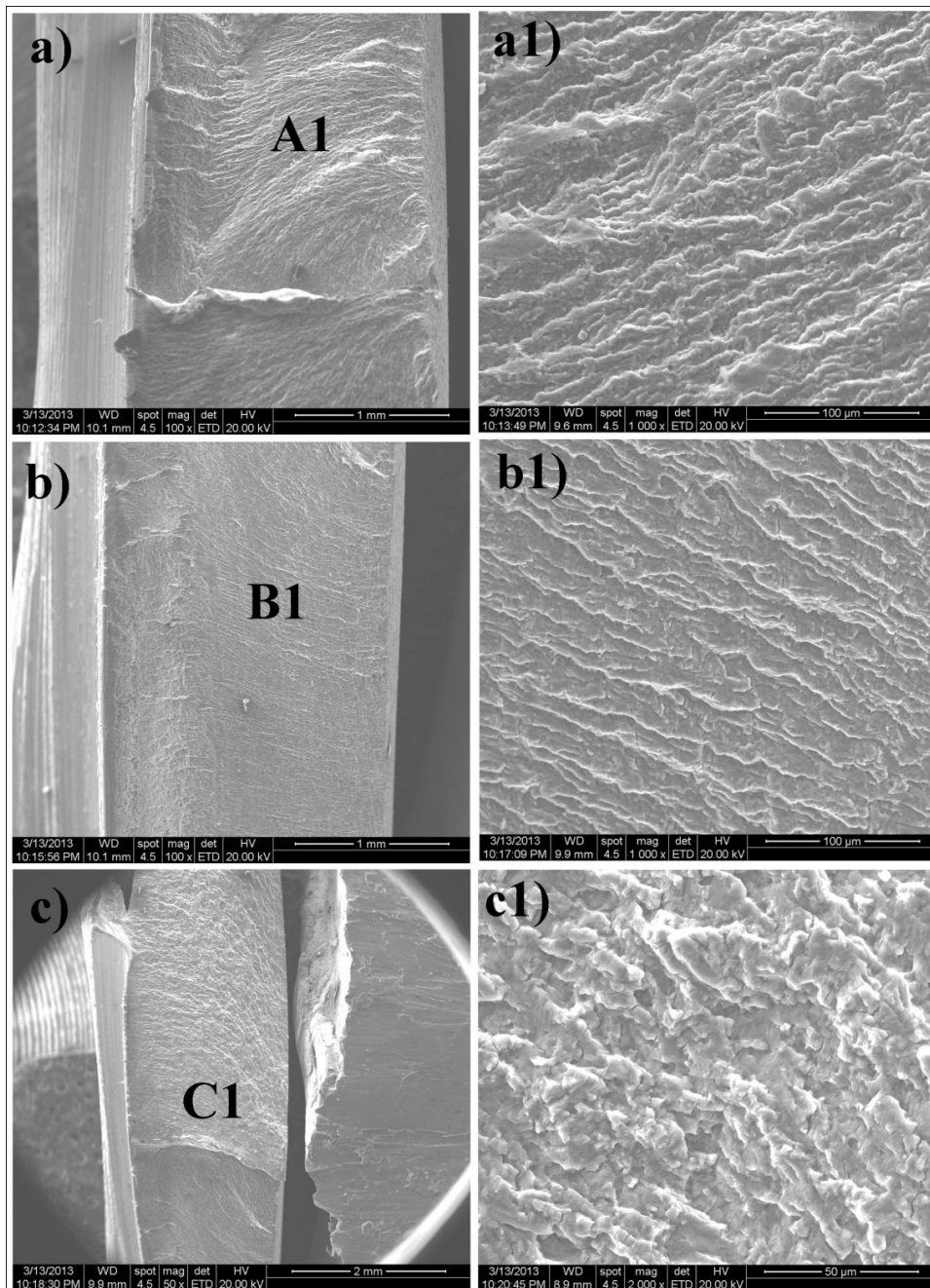
Fig. 8. Typical SEM micrographs of fracture surfaces in WFSSW joint (a), (b) and (c) fracture surface of upper sheet, (a1), (b1) and (c1) magnified views at points A1, B1, C1 in (a1), (b1) and (c1) respectively.

3.3 Fatigue test

Fig. 9 shows the relationship between the load range (N) and the number of cycles to failure in the WFSSW joints

made at a tool rotational speed of 900 rpm. The arrow mark at right bottom at the right bottom indicates that the specimens are not failed, but are terminated before failure. The weld specimens were terminated at 1.2×10^6 cycles. The transition of the fatigue crack growth behaviours from low cycle to high cycle fatigue indicated by dotted line. Note that the terminology here is defined based on the modes of fracture as explained earlier.
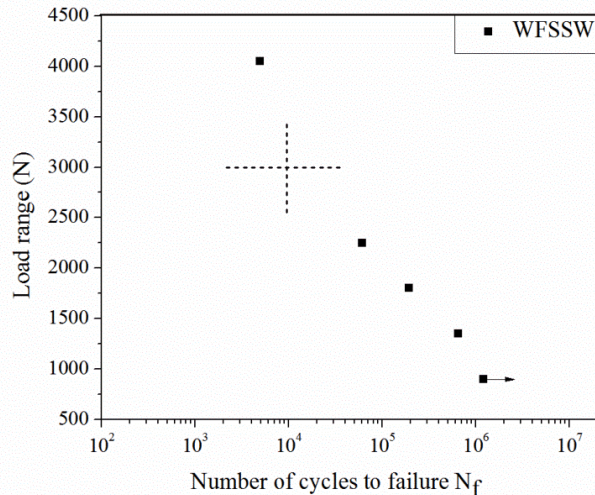

Fig. 9. Relationship between load range, and number of cycles to failure, N_f.

4. Conclusions

In this investigation, the effect of tool rotational speed on microstructure and mechanical properties of the WFSSW specimens of AA 6061-T6 sheets are analyzed by optical and scanning electron micrographs. The main results are summarized as follows.

1) Increasing the rotational speed from 900 rpm to 1800 rpm can generate coarse grains and decreasing the static shear strength.

2) The welds obtained at 900 rpm show the better static shear strength and found to be 8416 N.

3) The stir zones obtained in this experiment consist of very fine grain structure and show an increase in the Vickers hardness.

4) The hardness distribution of the welds exhibited a typical W-shape appearance and minimum hardness was obtained on heat affected zone (HAZ).

5) Optical and scanning electron micrographs of the welds after failure under quasi-static and cyclic loading conditions are examined. The micrographs show that the failure modes of the welds under low cyclic loading conditions are different from those welds under high cyclic loading conditions.

References

Agarwal, H., A.M. Gokhale, A.M., Graham, S., Horstemeyer, M.F., 2003. Void growth in 6061-aluminum alloy under triaxial stress state. Materials Science and Engineering A 341, 35-42.

Arbegast William, J., 2007, Friction stir welding and aircraft applications, Advanced Materials Processing Center (AMP), South Dakota School of Mines and Technology (SDSMT); June. <http://www.sdsmt.edu>.

Arul, SG., Miller, S.F., Kruger, G.H., Pan, T-Y., Mallick, P.K., Shih, A.J., 2008. Experimental study of joint performance in spot friction welding of 6111-T4 aluminum alloy. Science and Technology of Welding and Joining 13, 629–37.

Chowdhury, S.H., Chen, D.L., Bhole, S.D., Cao, X., Wanjara, P., 2012. Lap shear strength and fatigue life of friction stir spot welded AZ31magnesium and 5754 aluminum alloys. Materials Science and Engineering A 556, 500–509.

Jordon, J.B., Horstemeyer, M.F., Daniewicz, S.R., Badarinarayanan, H., Grantham, J., 2010. Fatigue characterization and modeling of friction stir spot welds in Magnesium AZ31 alloy. Transactions of the ASME. 041008-10, vol. 132, October 2010.

Lathabai, S., Painter, M.J., Cantin, G.M.D., Tyagi, V.K., 2006. Friction spot joining of an extruded Al–Mg–Si alloy. Scripta Materialia 55, 899–902.

Lin, P-C., Pan, J., Pan, T., 2008. Failure modes and fatigue life estimations of spot friction welds in lap-shear specimens of aluminum 6111-T4 sheets. Part 1: Welds made by a concave tool, International Journal of Fatigue 30, 74–89.

Malafaia, A. M. S., Milan, M.T., Oliveira, M. F., Spinelli, D., 2010. Fatigue behavior of friction stir spot welding and riveted joints in an Al alloy. Procedia Engineering 2, 1815-1821.

Mazda media release., 2003, Mazda develops world's first aluminum joining technology using friction heat; February 27, 2003. <http://www.mazda.com/publicity/release/0227e.html>.

Tozaki, Y., Uematsu, Y., Tokaji, K., 2007. Effect of tool geometry on microstructure andstatic strength in friction stir spot welded aluminium alloys. International Journal of Machine Tools and Manufacture 47, 2230–6.

Tran, V.-X. Pan, J., Pan, T., 2008. Fatigue behavior of aluminum 5754-O and 6111-T4 spot friction welds in lap-shear specimens. International Journal of Fatigue 30, 2175–2190.

Venukumar, S., Yalagi, S., Muthukumaran, S., 2013. Comparison of microstructure and mechanical properties of conventional and refilled friction stir spot welds in AA 6061-T6 using filler plate, Transactions of Nonferrous Metals Society of China 23, 2833-2842.

Zhang, Z., Yang, X., Zhang, J., Zhou, G., Xu, X., Zou, B., 2011. Effect of welding parameters on microstructure and mechanical properties of friction stir spot welded 5052 aluminum alloy. Materials design 32, 4461–4470.